

Review of the Physical Basis of Laboratory-derived Relations for Brittle Failure and their Implications for Earthquake Occurrence and Earthquake Nucleation

N. M. BEELER¹

Abstract—A laboratory-derived crack growth-based constitutive relation for brittle faulting is developed. The relation consists of two rheologic components, a nonlinear Arrhenius dependence of strain rate on temperature and stress, corresponding to subcritical crack growth, and a linear slip-weakening behavior associated with dilatancy, crack coalescence and supercritical crack growth. The implications of this general behavior for the onset of rapid slip- (earthquake nucleation) are considered. Laboratory observations of static fatigue and time-dependent failure from rock fracture and rock friction experiments are consistent with this simple constitutive description, as are the predictions of rate- and state- dependent equations for the onset of rapid frictional slip between bare rock surfaces. I argue that crack growth is the physical process that controls time-dependent rock fracture and the time-dependent onset of unstable frictional sliding. Some similar and related arguments made in the past 1/2 century in the fields of rock mechanics and earthquake seismology are reviewed. For stressing rates appropriate for the San Andreas fault system, the simple constitutive relation with lab-derived constants predicts a minimum time for nucleation of ~ 1 yr. General predictions are a minimum nucleation patch radius of 0.06 to 0.2 m, and a minimum earthquake moment of 8.5×10^7 Nm.

Key words: Earthquake nucleation, static fatigue, delayed failure, rate- and state-dependent friction.

1. Introduction

It has been nearly 40 years since BRACE and BYERLEE [1966] noted the similarity between repeating earthquake cycles and stick-slip sliding between bare surfaces of rock. In the intervening years earthquake research in rock fracture and rock friction has proceeded assuming that the onset of dynamic stress drop during laboratory rock failure or during frictional stick-slip experiments and the onset of earthquakes are controlled by the same underlying physical processes. Many significant advances have been made in rock friction, e.g., conditions where a fault responds unstably to changes in stress (e.g., DIETERICH, 1978; TULLIS and WEEKS, 1986), rate- and state- dependent constitutive relations to describe the lab observations (DIETERICH, 1979; RUINA, 1983; RICE and RUINA, 1983), and the mechanical conditions for frictional instability (RICE and RUINA, 1983; GU *et al.*, 1984). However, a significant limitation to laboratory-

¹ Brown University, Providence, Rhode Island. E-mail: Nicholas-Beeler@brown.edu

based relations, particularly rate and state equations which well describe rock friction under laboratory conditions, is that their exact physical basis is unclear. So long as particular laboratory-observed effects are empirical, i.e., not clearly attributed to thermally activated processes, it is difficult to extrapolate the observations in pressure and temperature to conditions other than those of the particular experiments, establish the dependence of the effects on environmental factors such as the presence of fluids and fluid chemistry, or to determine how the specific effects compare with others which might compete at significant depth in the earth.

This paper attempts to combine the essential experimental observations from brittle rock deformation into simple physically-based constitutive equations for earthquake nucleation. I argue that laboratory observations of rock fracture and rock friction relevant to earthquake occurrence and earthquake nucleation result from subcritical and supercritical crack growth, as has been suggested many times for failure of intact rock, probably first by SCHOLZ (1968b). A qualitative two-component constitutive description for rock fracture which results from considering the physics of crack growth is the same form as proposed by DIETERICH (1992, 1994) as a simplification of rate and state equations appropriate for describing the onset of rapid frictional slip between bare rock surfaces. Thus, I argue that crack growth underlies the rheology of unstable frictional slip between rock surfaces and the rheology of rock fracture. In the context of earthquake nucleation, considering frictional instability and rock failure as both resulting from crack growth is conceptually appealing because fractured rock and highly comminuted wear product are the most obvious of byproducts of brittle rock deformation. The equations resulting from the analysis presented herein, consistent with other recent process-based models of rock friction (LAPUSTA *et al.*, 2000; NAKATANI, 2001, RICE *et al.*, 2001), make specific predictions for the expected size and form of the temperature dependence of rheological parameters associated with earthquake nucleation, and might be used to predict how these effects will change with experimental configuration, the presence of fluids, and fluid chemistry. Using the simple constitutive equations and laboratory-derived model parameters I summarize new and review previously published predictions for earthquake occurrence and earthquake scale, in particular the duration of nucleation, nucleation zone size, and minimum earthquake size.

2. Simple Description of Brittle Deformation

To model the onset of rapid slip at low temperature I assume that all inelastic deformation requires cooperative slip and crack growth within a localized zone. Slip may occur between asperities on opposite sides of a fault, between particles in a fault gouge, or on previously fractured surfaces. Regions which are fractured by crack growth during deformation may be regions of intact rock in front of a propagating rupture (LOCKNER *et al.*, 1991), interlocking asperities on preexisting fault surfaces

(DIETERICH and KILGORE, 1994), or particles which form grain bridges in gouge layers (e.g., SAMMIS and STEACY, 1994). To characterize the net shear resistance at constant deformation rate I use an approach similar to that of MOGI (1962) and SAVAGE *et al.* (1996) where the shear resistance is

$$\tau_0 = \tau_f \frac{A_f}{A} + \tau_i \frac{A_i}{A}. \quad (1)$$

Here τ_f is the shear resistance to slip, τ_i is the shear stress necessary to break the unfractured material, A is the initial contacting area per unit mass of the deforming zone, and A_f and A_i are the area per unit mass of the slipping (fractured) region and the cross-sectional area per unit mass of the unfractured portions of the fault zone, respectively. Taking $A = A_f + A_i$, assume that the intrinsic resistance to slip is smaller than the resistance to crack growth, $\tau_f < \tau_i$ and that A is constant. During failure, weakening with progressive slip δ results from the increase of A_f at the expense of A_i . For example, for the propagation of a single circular crack, the cracked area increases as $A_f \propto \delta^2$. So in general the fault zones of interest are unable to sustain large shear strain without loss of strength, consistent with general definitions of brittle behavior. Here for simplicity, assume that crack area increases linearly with slip $A_f = C\delta$, where C is a constant with dimensions of length per unit mass. Using the definitions $\Delta\tau = \tau_i - \tau_f$ and $d_* = A/C$, equation (1) becomes

$$\tau_0 = \tau_i - \Delta\tau \frac{\delta}{d_*}. \quad (2)$$

This relationship (Fig. 1a) is consistent with laboratory observations of gradual slip-weakening during failure of intact rock (e.g., WONG, 1986) and stick-slip friction (e.g., OKUBO and DIETERICH, 1981; 1984) (Fig. 1b). Equation (2) is the slip-weakening form previously shown to be a useful general description of quasi-static and dynamic material failure (PALMER and RICE, 1973; IDA, 1972) that has been used extensively in cohesive zone models of shear fault propagation in the geophysical literature.

In previous implementations of slip-weakening the characteristic length d_* describes a gradual loss of material cohesion as in (2). However in many previous applications to earthquake mechanics, slip-weakening is used to model dynamic rupture propagation, that is, only super-critical behavior. In such applications the characteristic length has additional significance, principally, d_* is a model representation, related to the dimension of the region of yielding (the process zone) surrounding the tip of the propagating rupture. The size of the region surrounding the tip in which the stress is high enough to cause yielding increases with crack length or distance of propagation, implying that the process zone increases with the distance of crack propagation (ANDREWS, 1976). Thus, in models of large scale rupture propagation in the earth, the characteristic length should increase with displacement (ANDREWS, 1976). However, in this paper I am interested in the very small

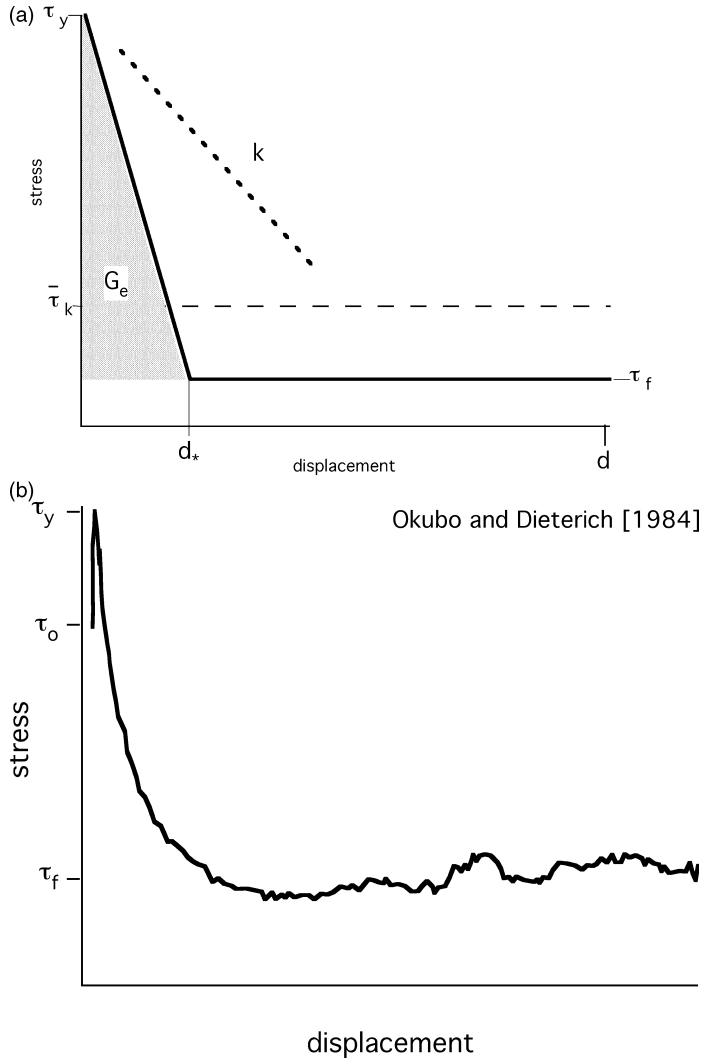


Figure 1

Slip-weakening relationship for fault strength drop. a) Idealized linear relationship after IDA (1972) and PALMER and RICE (1973). Strength drops from a peak (yield) τ_y to a residual level τ_f over a characteristic displacement d^* . The energy per unit area expended in dropping the strength $G_e = (\tau_y - \tau_f)d^*/2$, the effective shear fracture energy (shaded), can be equivalently expressed as $G_e = (\bar{\tau}_k - \tau_f)d$, where d is the total displacement and $\bar{\tau}_k$ is the displacement averaged fault strength. In this example, the initial displacement rate of strength drop (solid line), the slip-weakening rate $(\tau_y - \tau_f)/d^*$, is greater than the rate of stress drop (heavy dashed line) $k = d\tau/d\delta$ defining the conditions necessary for unstable, rapid slip. b) Laboratory observation of slip-weakening of a granite fault surface during dynamic strength drop at 3.45 MPa normal stress (OKUBO and DIETERICH, 1984).

displacements associated with earthquake nucleation; with reference to Figure 1, these displacements $\delta < d_*$ are the pre-peak and immediately post-peak displacements associated with the onset of rapid slip. Initially, I assume that d_* in the qualitative model (2) is constant. Later, in section 4.3 I consider implications of variable d_* for nucleation.

2.1 Slow Crack Growth

In brittle materials the resistance to crack growth depends positively on the growth rate while the growth rate is low. Figure 2 shows examples of this 'subcritical' behavior, rate data from single cracks propagating in selected quartzofeldspathic materials - fused silica glass (LAWN, 1993), synthetic quartz, and Westerly Granite (ATKINSON and MEREDITH, 1987). In Figure 2 the horizontal axis is crack propagation velocity and the vertical axis is the stress intensity K_I ; stress intensity is related to the remotely applied driving stress σ_r and to the crack length c as $K_I \propto \sigma_r \sqrt{c}$. Thus, as shown in Figure 2, subcritical fracture growth has a nonlinear viscous rheology; as the stress on the sample increases crack velocity increases, or alternatively, as the crack propagation velocity increases, the crack strength increases. Subcritical crack growth in minerals is generally similar to that in glass and at comparable temperature crystalline materials (quartz) are often somewhat stronger than their amorphous counterpart (fused silica). Note finally that there is a measurable temperature dependence to crack growth, indicating that a thermally activated mechanism controls growth. Arguably, subcritical crack growth occurs in all instances of natural faulting and in laboratory rock fracture and friction experiments as indicated by damage such as pervasive micro-cracks, macroscopic fracture, and wear material (gouge).

For well-studied minerals and for other brittle materials it is generally accepted that subcritical crack propagation rate is determined by the rate of chemical reaction at the crack tip, i.e., the rate at which bonds are broken at the tip (e.g., CHARLES and HILLIG, 1962; ATKINSON and MEREDITH, 1987). Descriptions of the chemical reaction rate v have the form

$$v = v_0 \exp\left(\frac{-E + \Omega\sigma_t - \Omega_m\Gamma/\rho}{RT}\right). \quad (3)$$

(CHARLES and HILLIG, 1962) where E is the stress free activation energy, Ω is the activation volume, Ω_m is molar volume, Γ is the interfacial energy, R is the gas constant (8.3144 J/mol K) and ρ is the radius of curvature at the crack tip. Note that as v increases, the crack tip strength σ_t increases. Using the substitutions $\Delta Q = E + \Omega_m\Gamma/\rho$ and $\sigma_0 = \Delta Q/\Omega$ (3) can be written

$$v = v_0 \exp\frac{-\Delta Q(1 - \sigma_t/\sigma_0)}{RT}. \quad (4)$$

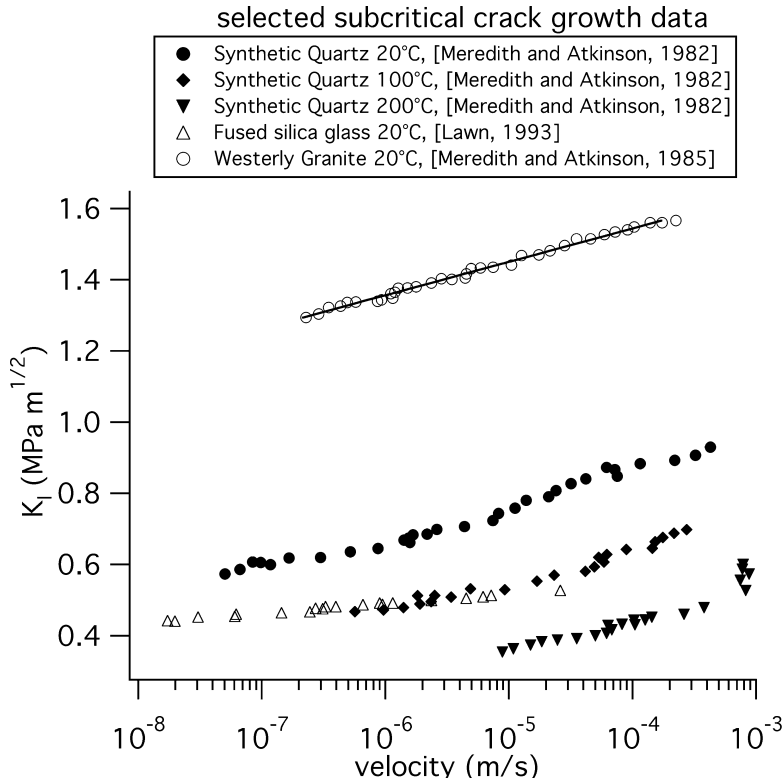


Figure 2

Subcritical crack growth in quartzofeldspathic materials. Crack stress intensity K_I versus velocity for fused silica glass (Lawn, 1993), synthetic quartz (ATKINSON and MEREDITH, 1987), and Westerly granite (ATKINSON and MEREDITH, 1987). The stress intensity is proportional to the remotely applied stress; thus the vertical axis reflects the driving stress for subcritical crack extension. Also shown is a fit to the granite data using $K_I = K_0 + (dK_I/d \ln V) \ln V$, with $dK_I/d \ln V = 0.041 \text{ MPa m}^{1/2}$.

Assume the rate of crack propagation is proportional to the reaction rate in (4). I further expect that the propagation velocity of a single crack, or the average propagation velocity of cracks within a localized fault zone to be proportional to the shear deformation rate across the fault zone so that $V = \alpha v$. Finally, assume that the remotely applied shear- stress driving crack propagation τ , equivalently macroscopic shear resistance of regions to fracture, reflects the intrinsic strength of the subcritical cracks within the region, $\sigma_t = \kappa \tau$. Here, κ is like a dimensionless stress intensity factor that depends on the geometry. However, unlike stress intensity, for simplicity I have arbitrarily assumed that κ is constant and does not depend on crack dimension, consistent with the crack growth experiments. After combining all of these assumptions the deformation rate is

$$V = V_0 \exp \frac{-\Delta Q(1 - \tau\kappa/\sigma_0)}{RT} \tag{5a}$$

where $V_* = v_0/\alpha$. Rearranging (5a) with V as the independent variable and using the substitutions $\tau_0 = \sigma_0/\kappa$ and $\zeta = RT\sigma_0/\Delta Q\kappa$ yields

$$\tau = \tau_0 + \zeta \ln \frac{V}{V_*}. \quad (5b)$$

Note that the resulting equation (5b) has the same form of stress dependence as the experimentally measured subcritical crack growth data (Fig. 2); stress depends logarithmically on the deformation rate with a coefficient ζ that is related to temperature and the thermal activation energy (also see, LAPUSTA *et al.*, 2000; NAKATANI, 2001; RICE *et al.*, 2001).

2.2 Simple Failure Equation

Combining the rate-independent relation for brittle deformation (2) with the accounting of the rate dependence of crack growth (5b) leads to a slip and slip rate dependent formulation

$$\tau = \tau_i + \zeta \ln \frac{V}{V_*} - \Delta\tau \frac{\delta}{d_*}. \quad (6a)$$

Observations from studies of rock friction (e.g., DIETERICH, 1981; TULLIS and WEEKS, 1986; BLANPIED *et al.*, 1998) and failure of intact rock (SCHOLZ, 1968a, b; LOCKNER, 1998), over a wide range of deformation rates are generally consistent with (6b); rock shear resistance at low temperature, low strain, and low strain rate depends weakly and logarithmically on the rate of inelastic deformation. Normalizing by normal stress yields a relation for friction, $\mu = \tau/\sigma_n$,

$$\mu = \mu_* + a \ln \frac{V}{V_*} - \frac{\Delta\tau\delta}{\sigma_n d_*}. \quad (6b)$$

Equation (6b) is the same form as a simplification, appropriate for representing the onset of rapid slip, suggested by DIETERICH (1992; 1994), of a particular rate and state variable constitutive equation widely used in studies of rock friction and earthquake mechanics (RUINA, 1983; LINKER and DIETERICH, 1992). Equivalence with (6a) requires $a = \zeta/\sigma_n$ and $\mu_* = \tau_i/\sigma_n$.

2.3 Expected Values of Coefficients

According to equation (6), strength during loading to brittle failure depends only on slip rate and slip. Expected values from laboratory experiments for the two coefficients a and, $\Delta\tau/\sigma_n d_*$ which control the respective dependencies, are listed in Table 1. Both friction and intact failure tests yield values of a ranging 0.003 to 0.009 for granite at low temperature. Agreement between a for friction and intact rock was found by TULLIS and WEEKS (1987) for carbonate rocks. In the case of granite, this similarity lead LOCKNER (1998) to suggest that subcritical crack growth is the

Table 1
Parameters for Granite

	Rate dependence	$\Delta\tau/\alpha_n d_*$	Reference
Friction	$\xi = 0.003\sigma_n$ to $0.009\sigma_n$	0.014 to $0.044/\mu\text{m}$	BLANPIED <i>et al.</i> (1998)
Friction			OKUBO and DIETERICH (1984)
Fracture	$\xi = 0.007\sigma_n$ to $0.009\sigma_n$ (20°C)	0.096×10^{-3} to $0.21 \times 10^{-3}/\mu\text{m}$	WONG (1986)
Fracture			LOCKNER (1998)
Crack growth	$dK_I/d \ln V = 0.041 \text{ MPa m}^{1/2}$ (20°C)	N/A	ATKINSON and MEREDITH (1987)

mechanism underlying this effect in both friction and rock failure of granite. While the rate dependence of shear strength from subcritical crack growth experiments in granite $dK_I/d \ln V = 0.041 \text{ MPa m}^{1/2}$ (Fig. 2, Table 1, data from ATKINSON and MEREDITH, (1987)) is available for comparison with friction tests at low normal stress, there are many complications in interpretation. The conclusion from friction and rock fracture tests is that a is a frictional quantity; that is, it does not depend on normal stress, requiring that ξ in (6) scales with normal stress. While this normal stress dependence of ξ is not included in the present qualitative model, it might be incorporated following the approach of LOCKNER (1993). An additional difficulty is that rate dependence inferred from ATKINSON and MEREDITH (1987) is crack length dependent and crack length is ignored in our treatment. At present no method of comparison between friction experiments and crack growth data has been established. A third difficulty is that $dK_I/d \ln V$ inferred from ATKINSON and MEREDITH (1987) applies to mode I (tensile) crack propagation; at high confining pressure appropriate for crustal shear faulting, shear and mixed mode crack propagation is expected and such subcritical crack growth measurements are not available. A final problem is that there are four regions of subcritical fracture growth, all with different rate dependence. The existing data for mode I in rocks and minerals correspond primarily to region 1 (ATKINSON and MEREDITH, 1987); it is unclear whether these are the appropriate data to compare to rock friction and rock failure tests. Given these unknowns, in the remainder of this study equation (6) is used with an empirically determined value of $a = 0.008$ appropriate for both granite friction and failure of intact granite (Table 1).

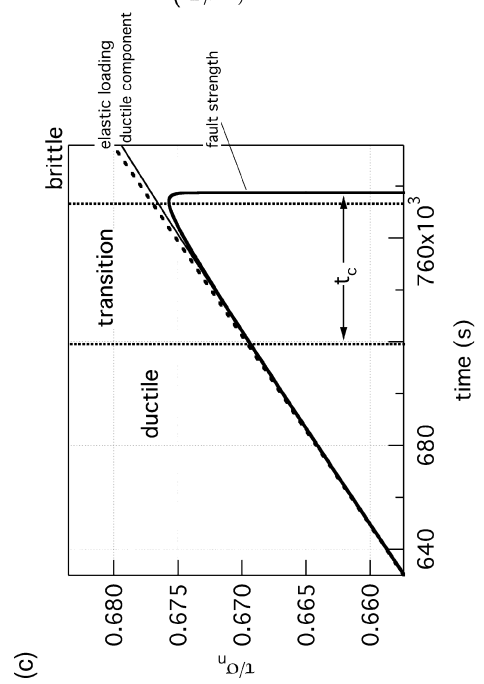
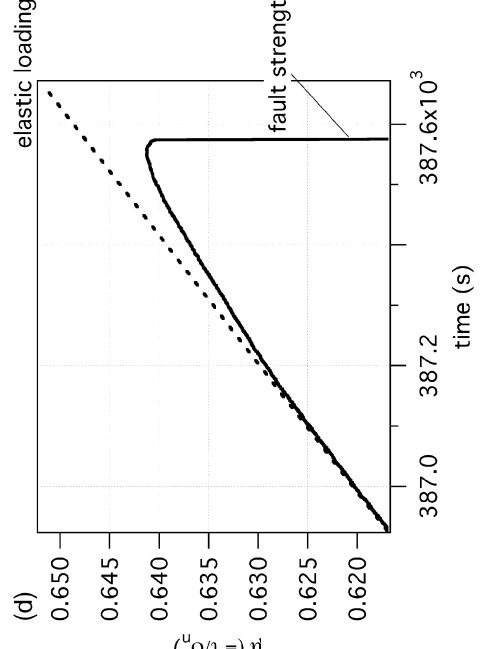
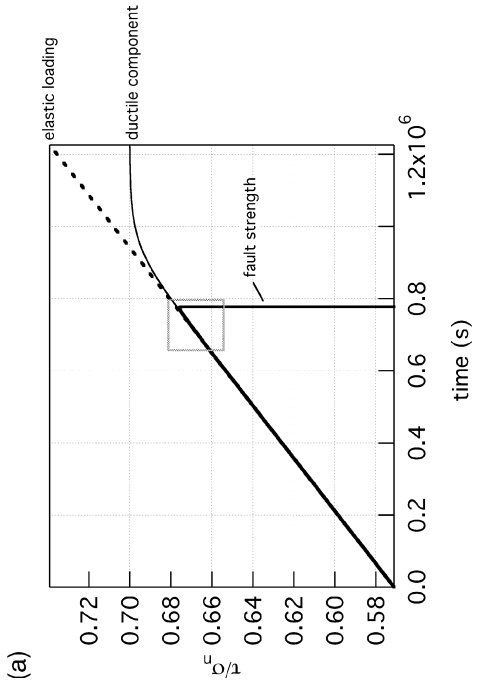
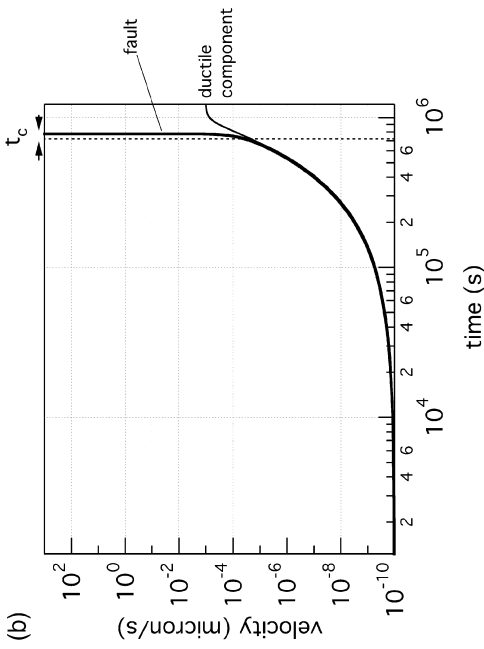
To infer values of the slip-weakening coefficient I use the slip-weakening strength drop (Fig. 1) from failure experiments on granite summarized by WONG (1986) and from granite stick-slip experiments of OKUBO and DIETERICH (1981). The slip-weakening component of (6b) can be equated with the dynamic strength drop from the experimental measurements, $\Delta\tau = (\tau_y - \tau_f)$ (Fig. 1). In both cases I estimate the effective dynamic strength drop from the measured shear fracture energy G_e and the

characteristic slip-weakening distance d_* according to $(\tau_y - \tau_f) = 2G_e/d_*$. Knowing the strength drop, normal stress and slip-weakening distance specifies the displacement rate of slip-weakening $(\tau_y - \tau_f)/\sigma_n d_*$. If d_* scales with A , the initial contact area per unit mass within the fault zone, then the slip-weakening coefficient $\Delta\tau/\sigma_n d_*$ should be very different for intact failure tests and friction. As friction involves areas of asperity contact which are typically a few percent or less of the total fault area, and intact failure involves fracture of the entire fault, d_* is expected to be two to three orders of magnitude larger for intact rock failure. Thus, excepting differences in stress drop $\Delta\tau$, the slip-weakening component $\Delta\tau/\sigma_n d_*$ should be about two to three orders of magnitude larger for friction than it is for intact failure. This is consistent with the observations (Table 1); the representative displacement rate of slip-weakening for fault slip in terms of friction is $0.029/\mu\text{m}$ whereas for rock fracture it is $0.00015/\mu\text{m}$.

However, $\Delta\tau$ and d_* are probably coupled. For rock fracture the “fault” initially is as strong as the surroundings, having the strength of intact rock. On the other extreme, simulated laboratory faults are weak with respect to the surrounding rock and are cohesionless and artificially flat except at small wavelengths. Thus the strength drop for rock fracture should exceed that for friction. Similarly, the amount of strain necessary to weaken intact rock exceeds that necessary to break asperities on a laboratory fault surface. Natural seismic faults should have roughness much greater than in laboratory friction experiments (POWER *et al.*, 1987), and have non-zero cohesion less than that of intact rock. Considering the displacement rate of slip-weakening from laboratory friction and laboratory rock fracture experiments as end members, I use a value intermediate between the two different types of laboratory tests, $\Delta\tau/d_*\sigma_n = 0.002$ to $0.003/\mu\text{m}$ in applying laboratory results to model earthquake nucleation and small earthquakes.

3. Physical Characteristics, Significance, Interpretation

If one allows that earthquake occurrence involves crack growth at some scale, constitutive models for failure must involve two components, a ductile response at small strains, represented in (6b) by the rate-dependent term $a \ln V/V_*$, and a brittle response at large strain represented by the slip-weakening term $-\Delta\tau\delta/\sigma_n d_*$, in (6b). The implied behavior is easily illustrated; consider a fault loaded at a constant displacement rate V_L (Fig. 3a); for small values of slip, $\delta \ll d_*\sigma_n/\Delta\tau$, the third term on the right-hand side of (6b) is negligible and the second term dominates. That is, at small inelastic strains the fault strength depends positively on deformation rate, and the fault is ductile in the classic sense that strain can be accommodated without loss of strength. The ductile component of (6b) $\mu = \mu_* + a \ln V/V_*$ characterizes temporal variation of slip rate very well over most of the loading to failure (Fig. 3b). During this time, labeled ductile in Figure 3c, the sliding velocity increases (Fig. 3b), and yet the stress on the fault also increases (Figure 3a and 3c). As more strain accrues, the third



term of (6b) becomes significant and leads to a deviation from a linear (elastic) increase in shear stress τ with time t (Figure 3a and 3c); shear stress on the fault is $\tau = k(V_L t - \delta)$, where k is the stiffness of the surroundings. In this transition stage the slip rate also deviates from the ductile curve (Figure 3b). Eventually the slip weakening term in (6b) dominates, resulting in truly brittle behavior at large strains, and subsequently rapid stress drop occurs. Figure 3d depicts a laboratory example of this gradual onset of failure, loading of a granite fault at 50 MPa confining pressure at $V_L = 0.1 \mu\text{m/s}$ (BEELER and LOCKNER, 2003). Thus the crack-based model of faulting, and the laboratory observations on which it is based, exhibit delayed failure—a lag time between the onset of detectable slip, or the time of peak stress, and the time of failure.

The ductile response represents the stable growth of subcritical cracks while the eventual brittle response reflects critical and super-critical crack growth, the coalescence of previously isolated cracks, dilatancy and the associated loss of material cohesion. More sophisticated two-component models for rock fracture, based on the same conceptual approach taken in the previous section, are common in the international rock mechanics and fracture mechanics literature dating back at least to the 1960s (e.g., ZHURKOV, 1965; ZHURKOV *et al.*, 1977).

4. Implications for Time of Earthquake Occurrence

4.1 Static fatigue and delayed failure

As reflected in equation (6b) and in laboratory experiments, neither rock failure nor frictional instability occur at a threshold stress. This is well illustrated by the



Figure 3

Characteristics of laboratory failure during loading at a constant rate. Parts a) – c) show the results of simulations with equation (6b) where the fault is loaded elastically $d\tau/dt = k(V_L - V)$ with $V_L = 0.001 \mu\text{m/s}$, stiffness $k/\sigma_n = 0.000137/\mu\text{m}$, $\mu^* = 0.7$, $a = 0.008$, $\Delta\tau/\sigma_n d^* = 0.0024/\mu\text{m}$, and initial velocity $V_s = 1.0 \times 10^{-10} \mu\text{m/s}$ at $t = 0$. a) Shear stress in the plane of the fault in the shear direction versus time. Shown are the elastic loading $d\tau/dt = kV_L$ that would result if the fault did not slip (dashed), the ductile component of the failure relation $\tau/\sigma_n = \mu^* + a \ln V/V^*$ (black) and the complete solution to (6b) (heavy black). The gray box denotes the region shown in Figure 3c. b) Sliding velocity versus time for the calculation shown in Figure 3a. The ductile component of the failure equation is shown for comparison (black). During most of the loading time the fault behavior is well described by the ductile solution because the total displacement is extremely small and the slip weakening term $\Delta\tau\delta/\sigma_n d^*$ in (6b) is negligible. c) Blow up of gray box in Figure 3a. The elastic loading (dashed) and ductile component of the failure relation are shown again for comparison. Also shown are the approximate boundaries (dotted lines) between the ductile and brittle regions of (6b). The onset of truly brittle behavior occurs at the peak stress when $V = V_L$. An approximation to the upper limit of truly ductile behavior is shown (see discussion in section 4.3). Over the duration of time labeled transition, the fault shows mixed behavior; it strengthens as the sliding rate increases but is weaker than the purely ductile component. d) Actual laboratory observation of the onset of unstable sliding between surfaces of Westerly granite at 50 MPa confining pressure and $V_L = 0.1 \mu\text{m/s}$ (BEELER and LOCKNER, 2003).

laboratory observed phenomenon known in mechanical engineering, material science, and rock mechanics as ‘static fatigue’ or ‘stress corrosion’—an inherent time delay between the application of a stress increase and the occurrence of brittle failure induced by the stress change (e.g., SCHOLZ, 1972; KRANZ, 1980). Here and throughout I refer to changes in the fault shear stress τ using the normalized frictional stress $\mu = \tau/\sigma_n$ (6b). To consider static fatigue of (6b), take the temporal derivative and equate it to zero. If stress is raised to a particular level μ_s at time $t=0$ and then held constant, the sliding rate evolves from the starting velocity V_s at $t=0$ according to

$$V = \frac{V_s a \sigma_n d_*}{a \sigma_n d_* - \Delta \tau t V_s} \quad (7a)$$

where $V_s = V_* \exp([\mu_s - \mu_*]/a)$ (Fig. 4a). The delay time t_d between the application of the stress that induces failure and actual time of failure is

$$t_d = \frac{a \sigma_n d_*}{\Delta \tau V_*} \exp([\mu_* - \mu_s]/a) \quad (7b)$$

The relationship between stress change and the delay time is such that the larger the stress level, the sooner the induced failure event (Fig. 4b). Thus, if earthquake failure is controlled by the same processes as in laboratory rock failure and frictional instability experiments, the failure time of an earthquake triggered by a particular stress change depends on the size of stress change and on how close the fault is to failure prior to the stress change (proximity to failure). That rock failure time is related to stress change in this general way has been known since GRIGGS (1936). Figure 4c shows a laboratory example of the typical static fatigue behavior of rock, rock fracture of granite at 53 MPa confining pressure (KRANZ, 1980).

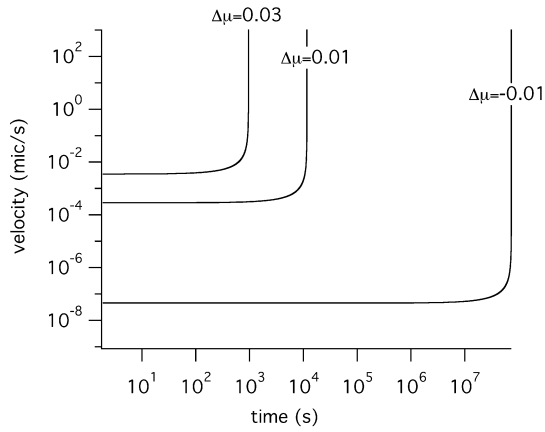
As the relationship between stress change and failure time is nonlinear, when one considers populations of faults with an initially random distribution of proximity to failure, a stress change produces a seismicity rate due to triggered events that is initially very high and decreases with time following the stress change. This is the behavior seen in induced acoustic emissions, microseismicity, and Omori aftershock sequences, as was noted by MOGI (1962), and subsequently by many researchers (e.g.,



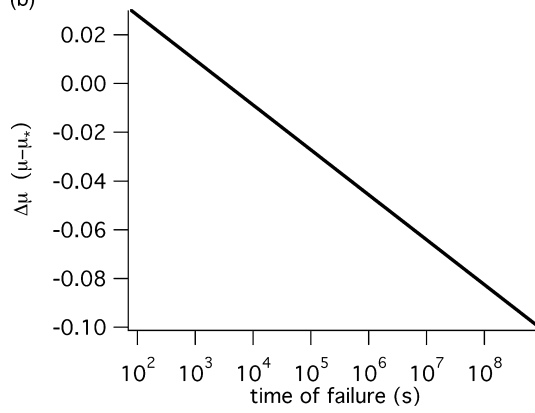
Figure 4

Static fatigue characteristics. Parts a) and b) are simulations using equation (6b) with $\mu_* = 0.7$, $V_* = 0.001 \mu\text{m/s}$, $a = 0.008$, and $\Delta\tau/\sigma_n d_* = 0.0024 / \mu\text{m}$. In a static fatigue test, the fault shear stress is raised from zero to μ_s nearly instantaneously. In this simulation, the level of stress fixes the initial velocity $V_s = V_* \exp([\mu_s - \mu_*]/a)$. a) Slip velocity with time as given by equation (7a). Shown are three cases corresponding to $\Delta\mu = \mu_s - \mu_* = 0.03, 0.01$ and -0.01 . The higher the stress relative to the reference μ_* , the higher the initial slip rate and the sooner failure occurs. b) The time of failure t_d versus the stress level for a series of simulated static fatigue tests as specified by equation (7b). c) Actual experimental static fatigue data from rock fracture of granite at 53 MPa confining pressure (KRANZ, 1980). Failure stress was converted to friction assuming a 30° angle between the greatest principal stress and the incipient failure plane. $\Delta\mu$ was calculated using μ at 10^4 s as the arbitrary reference μ_* .

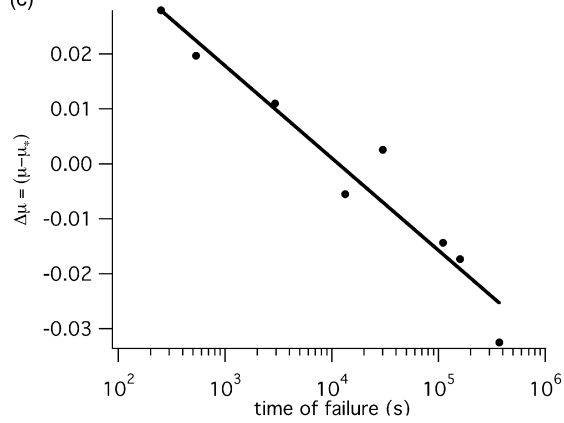
(a) fatigue characteristics of simple fault failure relation



(b)



(c)



SCHOLZ, 1968b; KNOPOFF, 1972; DAS and SCHOLZ, 1981; YAMASHITA and KNOPOFF, 1987; HIRATA, 1987; REUSCHLE, 1990; and MARCELLINI, 1995, 1997 among others). Furthermore, many of these authors have developed fracture growth based models of aftershocks; successful modeling of aftershocks, foreshocks and general seismicity rate changes with (6b) by DIETERICH (1994) and DIETERICH *et al.* (2000) being a recent, general and significant advance.

4.2 The Characteristic Time

Because the small strain behavior of equation (6b) is ductile, this equation exhibits a characteristic time. Consider constant rate elastic loading of a fault where the loading rate represents tectonic stressing $d\tau/dt = k(V_L - V)$. At small strain the rate of stress change of equation (6b) is $d\tau/dt \approx a\sigma_n dV/VdV$. Combining these two expressions and integrating yields

$$\frac{1}{V} \approx \left(\frac{1}{V_s} - \frac{1}{V_L} \right) \exp\left(-\frac{\dot{\tau}}{a\sigma_n} t \right) + \frac{1}{V_L}$$

where V_s is the velocity at $t = 0$, and $\dot{\tau} = kV_L$. Thus, slowness (V^{-1}) is exponential with a characteristic time $t_c = a\sigma_n/\dot{\tau}$. This constant loading rate, characteristic time figures prominently in applications of (6b) to earthquake nucleation and earthquake occurrence as I summarize next.

4.3 The Duration of Nucleation

The simple failure equation (6b) has a number of analytical solutions for simple stressing histories that are useful for analysis of earthquake occurrence, earthquake rate, and precursory slip (DIETERICH, 1992, 1994; GOMBERG *et al.*, 1998). For predicting earthquake failure time under a constant rate of stressing $\dot{\tau}$ due to plate motion, time until failure depends only on the sliding velocity

$$t_{fj} = \frac{a\sigma_n}{\dot{\tau}} \ln \left[\frac{\dot{\tau}}{\gamma V} + 1 \right]. \quad (8a)$$

where $\gamma = (\Delta\tau/d_* - k)$ and k is the elastic stiffness (DIETERICH, 1994) (Fig. 5a). During most of the loading, the fault slip velocity is small but as the stress rises slip rate becomes significant. Similarly, the total accrued displacement prior to failure is exceedingly small and only becomes appreciable near the time of failure

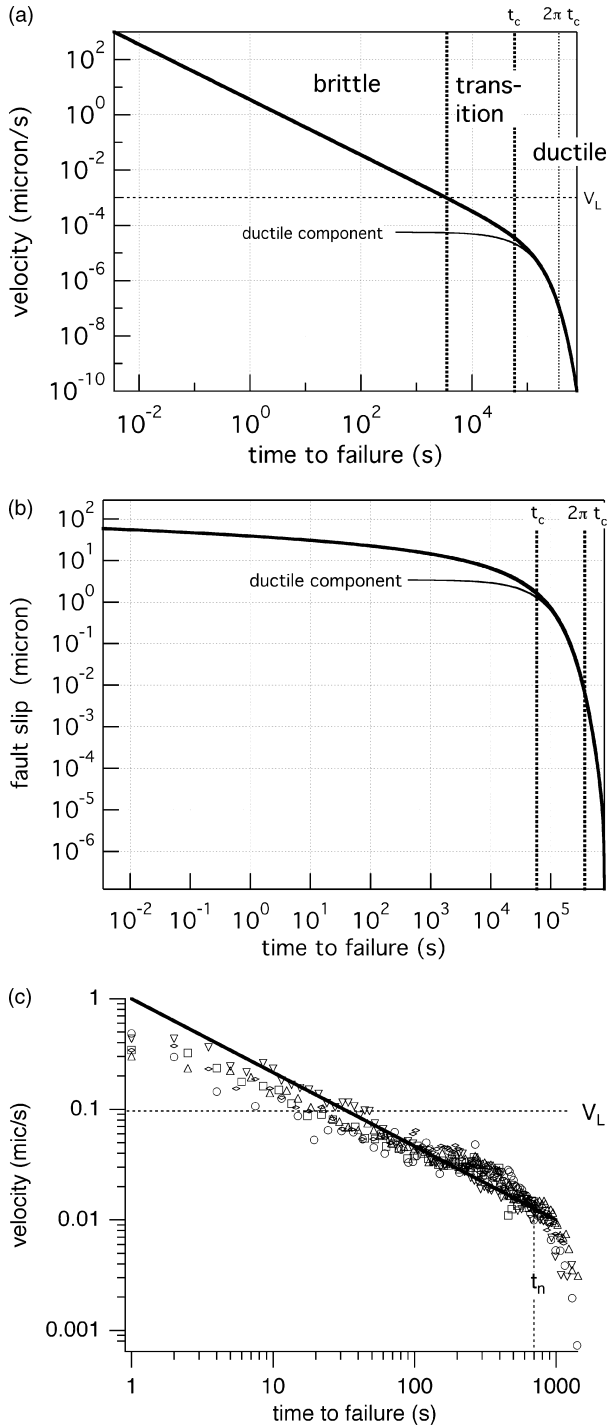
$$\delta = -\frac{a}{\gamma} \ln \left[1 - \frac{\gamma V_s}{\dot{\tau}} \left\{ \exp\left(\frac{\dot{\tau} t}{a\sigma_n} \right) - 1 \right\} \right]. \quad (8b)$$

(DIETERICH, 1992, 1994; GOMBERG *et al.*, 1998) where V_s is the velocity at $t=0$ (Fig. 5b). Whether or not the fault is slipping at an appreciable rate directly reflects the expected tradeoffs between the two rheologic components of (6b). With reference to Figure 5a, time between the change from steep to shallow slope and the failure

time is marked by the time at which the full solution of (6b) deviates from the ductile component of (6b). This time can be thought of as the duration of nucleation, the time during which the fault is undergoing appreciable precursory slip. The duration of nucleation is effectively independent of the slip-weakening component $-\Delta\tau\delta/\sigma_n d_*$ of equation (6b), as is shown in constant loading rate calculations with $\Delta\tau\delta/\sigma_n d_*$ varying over 4 orders of magnitude (Fig. 6). The nucleation time therefore is controlled entirely by the ductile component of (6b) $a \ln V/V_*$ and depends only on a . Furthermore, the nucleation time is on the order of the characteristic time of $a\sigma_n/\dot{\tau}$. t_n has been approximated as $t_n = t_c = a\sigma_n/\dot{\tau}$ by DIETERICH (1994) and as $t_n = 2\pi t_c = 2\pi a\sigma_n/\dot{\tau}$ by BEELER and LOCKNER (2003). These estimates of t_n seem to bound the actual value well (Figs. 5a and 6).

In addition to being the effective duration of nucleation, t_n is the predicted duration of Omori-like aftershock sequences for fault populations obeying (6b) (DIETERICH, 1994). Why the duration of an aftershock sequence is related to the nucleation time can be understood by noting that for constant loading rate t_n is the maximum possible delay between the onset of appreciable slip and the time of failure (Fig. 5b). Therefore for faults that are initially closer to failure than t_n , a small stress change changes the sliding velocity and shortens the delay time by an amount that depends on the initial time to failure. However for faults initially much farther from failure than t_n , a small stress change changes the sliding velocity but will not shorten their delay time. As a result, the seismicity rate at times greater than t_n after a static stress change, is the same as the seismicity rate prior to the stress change (DIETERICH, 1994). t_n is also the expected period of time over which earthquake occurrence rates should be insensitive to continuous small amplitude stress changes such as the solid earth tides (BEELER and LOCKNER, 2003). That the nucleation time determines whether earthquake occurrence is sensitive to tidal stresses can be understood again by noting that t_n is the maximum possible delay time. For an increase in stress of a period considerably longer than t_n , the nucleation time is negligible in comparison to the period; under these circumstances failure is effectively instantaneously triggered by the stress change, and there is a strong correlation between stress change and failure time. At periods shorter than t_n , failure is delayed due to the damping term $a \ln V/V_*$ and the correlation between small stress changes and seismicity rate is very weak (KNOPOFF, 1964; BEELER and LOCKNER, 2003).

To evaluate expected values of t_n for the San Andreas fault system assume a 10 MPa stress drop and recurrence intervals between 30 and 100 years (appropriate for large earthquake recurrence) ($\dot{\tau} = 1.0 \times 10^{-8}$ to 3.17×10^{-9} MPa/s), a depth range of 5–15 km with $\sigma_n = 18$ MPa/km (appropriate for hydrostatic fluid pressure), and an experimentally derived value of $a=0.0045$ (BEELER and LOCKNER, 2003) ($a\sigma_e=0.4$ – 1.2 MPa). Using $t_n = t_c$ the predicted duration is 1.2 to 12 years and for $t_n = 2\pi t_c$ the typical duration is 7.6 to 76 years. These values are consistent with some aftershock sequence durations and the absence of obvious tidal triggering by the



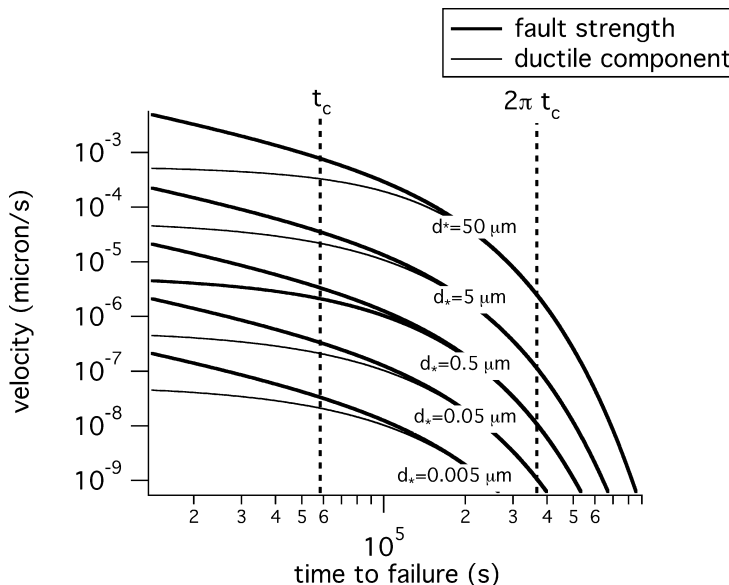


Figure 6

Time to failure characteristics of the simple brittle failure relation equation (6b) during loading at a constant rate for different values of the characteristic length d_* , as labeled. The fault (heavy curves) is loaded elastically $d\tau/dt = k(V_L - V)$ with $V_L = 0.001 \mu\text{m/s}$, stiffness $k/\sigma_n = 0.000137/\mu\text{m}$, $\mu_* = 0.7$, $a = 0.008$ and initial velocity $V_s = 1.0 \times 10^{-10} \mu\text{m/s}$ at $t = 0$. Various values of the ratio $\Delta\tau/\sigma_n d_*$ are used. The curve labeled $d_* = 5 \mu\text{m}$ corresponds to $\Delta\tau/\sigma_n d_* = 0.0024 \mu\text{m}$. Also shown is the ductile component of (6b) $\tau/\sigma_n = \mu_* + a \ln V/V_*$. For a particular value of d_* , the intersection of the heavy black and black curves is the duration of nucleation; the 4 sets of curves show that the duration of nucleation is essentially independent of d_* . Also shown are the two estimates of nucleation duration, the characteristic time $t_c = a\sigma_n/\dot{\tau}$ and $2\pi a\sigma_n/\dot{\tau}$.

solid earth tides. However, though shorter aftershock sequences may be evidence of low effective normal stress (super-hydrostatic pore pressure), smaller stress drops, higher stressing rates, or smaller values of a , aftershock durations can be much less



Figure 5

Time to failure characteristics. Parts a) and b) are simulations using equation (6b) during loading at a constant rate. The fault is loaded elastically $d\tau/dt = k(V_L - V)$ with $V_L = 0.001 \mu\text{m/s}$, stiffness $k/\sigma_n = 0.000137/\mu\text{m}$, $\mu_* = 0.7$, $a = 0.008$, $\Delta\tau/\sigma_n d_* = 0.0024 \mu\text{m}$, and initial velocity $V_s = 1.0 \times 10^{-10} \mu\text{m/s}$ at $t = 0$. a) Slip velocity versus time to failure. At high velocity, time to failure is inversely related to slip velocity; this behavior characterizes the mixed and brittle behavior of (6b). At very low velocity, the behavior is well described by the ductile component of (6b) $\dot{\tau}/\sigma_n = \mu_* + a \ln V/V_*$ (black). The upper boundary of ductile behavior is well approximated by the characteristic time $t_n = a\sigma_n/\dot{\tau}$ (heavy dotted line labeled t_c). Another estimate of the limit of ductile behavior $t_n = 2\pi a\sigma_n/\dot{\tau}$ is shown (dotted line). b) Displacement versus time to failure for the same calculation as shown in a). c) Actual laboratory observation of slip velocity versus time to failure for 5 successive slip events on a granite fault at 50 MPa confining pressure and $V_L = 0.1 \mu\text{m/s}$ (BEELER and LOCKNER, 2003], after DIETERICH and KILGORE [1996]. The solid line denotes a slope of -1 , and the dashed line t_n is an estimate of the duration of nucleation.

than 12 to 76 years and some are on the order of weeks or months. Further analysis with (6b) of aftershock sequences and of reported correlation between stress changes due to oceanic tides and earthquake occurrence (e.g., WILCOCK, 2001) may provide constraints on t_n that are not available from existing laboratory experiments.

5. Implications for Earthquake Size

On a planar fault loaded at a constant rate, slip with the fault strength (6b) can be inherently unstable to perturbations in slip or slip velocity. Some spatial aspects of the behavior can be illustrated with static calculations, principally, the expected spatial size of a nucleating earthquake. Consider an arbitrary distribution of slip on a planar fault in plane strain. The spatial distribution of shear stress $\tau(x)$ due to slip $\delta(x)$ is

$$\tau(x) = \frac{G}{2\pi(1-v)} \int_{-\infty}^{\infty} \frac{-d\delta/dx(x')}{x-x'} dx' \quad (9)$$

(WEERTMAN, 1979). The temporal derivative of (9)

$$\frac{d\tau(x)}{dt} = \frac{G}{2\pi(1-v)} \frac{d}{dt} \left(\int_{-\infty}^{\infty} \frac{-d\delta/dx(x')}{x-x'} dx' \right) \quad (10a)$$

can be evaluated using Leibniz's Rule to find

$$\frac{d\tau(x)}{dt} = \frac{G}{2\pi(1-v)} \int_{-\infty}^{\infty} \frac{-d(d\delta/dx(x'))}{dt} \frac{1}{x-x'} dx' \quad (10b)$$

Noting that, $d(d\delta/dx)/dt = d(d\delta/dt)/dx$, (10b) can be expressed as

$$\frac{d\tau(x)}{dt} = \frac{G}{2\pi(1-v)} \int_{-\infty}^{\infty} \frac{-dV/dx(x')}{x-x'} dx' \quad (10c)$$

Now consider a single wavelength perturbation above a uniform sliding speed V_0 , $V(x) = V_0(1 - A \cos \omega x)$ where the wavelength is $2\pi/\omega$. The spatial derivative of velocity is $dV/dx(x) = V_0 \omega A \sin \omega x$ and so long as there is only a single perturbation, the upper and lower integration limits of (10c) can be replaced by 2π and 0, respectively,

$$\frac{d\tau(x)}{dt} = \frac{G}{2\pi(1-v)} \int_0^{2\pi} \frac{-V_0 \omega A \sin \omega x'}{x-x'} dx' \quad (11a)$$

The temporal derivative of (6b) can be rearranged to give

$$\frac{dV}{dt}(x) = \frac{V(x)}{a} \left(\frac{1}{\sigma_n} \frac{d\tau}{dt}(x) + \frac{\Delta\tau V(x)}{\sigma_n d_*} \right) \quad (11b)$$

When (11a) is substituted into (11b), equation (11b) gives the spatial distribution of instantaneous slip acceleration of the perturbed fault patch, a measure of the growth rate. To determine the characteristic wavelength the procedure is to consider the growth rate of patches of different wavelength. Figure 7 shows that the spatial distribution of growth rate depends on the wavelength with the most uniform growth rate associated with a half wavelength ($l_c = \lambda/2$) $l_c = Gd_*/\Delta\tau$ (heavy solid line, Fig. 7). For this choice of parameters (see figure caption) $l_c = 0.5$ m. This particular wavelength should grow and maintain approximately constant shape whereas larger and smaller patches will either spread to larger or shrink to smaller wavelengths. Thus, earthquake nucleation on faults with (6b) should show a dominant nucleation patch size l_c . Time dependent calculations by DIETERICH (1992) using the same geometry as employed here show similar behavior. DIETERICH finds that during nucleation, patches with half-length greater than l_c shrink to l_c as slip accelerates, and slip perturbations of smaller wavelength tend to become smooth and coalesce to longer wavelength patches. However, in time-dependent calculations l_c is somewhat larger than inferred from static analysis; DIETERICH (1992) reports $l_c = 1.7Gd_*/\Delta\tau$ as the patch approaches dynamic slip speeds.

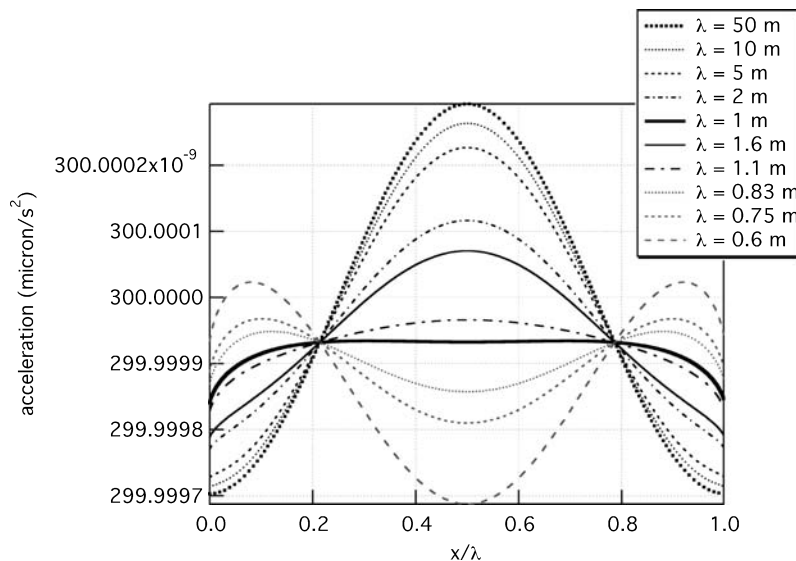


Figure 7

The spatial distribution of instantaneous slip acceleration on patches of a planar fault. Patches with a slip velocity perturbation of the form $V(x) = V_0 (1 - A \cos \omega x)$ were calculated with equations (11a) and (11b) using different wavelengths $\lambda = 2\pi/\omega$ for $\mu^* = 0.7$, $a = 0.008$, $\Delta\tau/\sigma_n d^* = 0.0024$ / μm , $\sigma_n = 21$ MPa, $G = 2.5 \times 10^4$ MPa, $\nu = 0.25$, $A = 0.5 \times 10^{-6}$ m/s, and $V_0 = 1 \times 10^{-6}$ m/s. The calculated distribution of growth rates depends on the wavelength. The most uniform growth rate being associated with a half wavelength ($l_c = \lambda/2$) $l_c = Gd_*/\Delta\tau = 0.5$ m.

5.2 Minimum Earthquake Nucleation Size

The minimum earthquake nucleation size can be estimated with a simpler geometry than used in the previous section; for example a fixed length static slipped patch (DIETERICH, 1986). Unstable sliding is only possible if fault strength drops so that stored elastic energy from the surrounding rock can be used to drive further slip. If an increment of slip on the fault surface reduces the fault strength faster than the driving stress is reduced, an unstable condition develops in which fault slip can accelerate into an earthquake and some of the stored elastic energy is radiated as seismic waves. If the elastic stiffness of the loading system is expressed as $k = d\tau/d\delta$, then the requirement for instability at constant normal stress is a critical stiffness (DIETERICH, 1979) $k_c = \sigma_n d\mu/d\delta$. For (6b) slip instability occurs for $k < k_c \approx \Delta\tau/d_*$ (DIETERICH, 1992) (Fig. 1). Using a circular crack of constant stress drop, the stiffness is $k = 7\pi G/16r$. For this circular patch, earthquake nucleation with (6b) is associated with patches of minimum radius $r_c = 7\pi G d_*/16\Delta\tau$. For $G = 2.5 \times 10^4$ MPa, an intermediate value of the ratio $\Delta\tau/d_*\sigma_n = 0.002/\mu\text{m}$ (see section 2.3) and effective normal stress between 90 and 270 MPa (effective normal stress gradient of 18 MPa/km over 5 to 15 km depth), the expected critical patch radii is between 0.06 and 0.2 meters. Nucleating slip on patches of this size would not be detectable at 7 km from the source even with the most sensitive instruments currently available (e.g., borehole strain meters) (JOHNSTON and LINDE, 2002). A more rigorous discussion and analysis of precursory strain and moment is given by DIETERICH (1992). Given that surface and space-based strain measures are much less sensitive to slip at depth than borehole instruments, the laboratory observations imply that precursory strain of earthquakes can only be measured in deep boreholes adjacent to seismic faults (also see, LORENZETTI and TULLIS, 1989).

5.3 Minimum Earthquake Size

Laboratory observations of frictional slip also imply a minimum earthquake size. Comparisons between lab, mining-induced events and other small earthquakes by MCGARR (1994; 1999) indicate that all are energetically similar, implying that fracture energy and radiated energy can be treated as scale-independent percentages of the available energy, at least for small events. Lab stick-slip events (OKUBO and DIETERICH, 1981; LOCKNER and OKUBO, 1983) have ratios $d_*/\Delta\delta_s \approx 0.1$ and the laboratory observed dynamic strength drops are frictional ($(\tau_y - \tau_f)/\sigma_n$ constant) with $(\tau_y - \tau_f)/\sigma_n = 0.09$ (WONG, 1986); using these values to determine the slip weakening coefficient $\Delta\tau/d_*\sigma_n$ leads to $\Delta\delta_s \approx 0.9\sigma_n d_*/\Delta\tau$. A lab-derived intermediate value for the slip-weakening coefficient, $\Delta\tau/d_*\sigma_n = 0.002/\mu\text{m}$ predicts a minimum-sized earthquake to have seismic displacements $\Delta\delta_s \approx 450\mu\text{m}$.

For a circular crack, the relationship between radius, static stress drop $\Delta\tau_s$ and seismic slip $\Delta\delta_s$ is $r = 7\pi G \Delta\delta_s/16\Delta\tau_s$. Taking the estimate $\Delta\delta_s = 0.45$ mm and a range of static stress drops 0.1 to 10 MPa yields $r = 155$ to 1.55 m. The seismic

moment M_o of a circular rupture of radius r is $M_o = G\pi r^2 \Delta\delta_s$, and the lab-estimated values of r and $\Delta\delta_s$ yield $M_o = 8.5 \times 10^{11}$ to 8.5×10^7 Nm. The minimum seismic moment from the smallest friction dominated mining-induced events reported by RICHARDSON and JORDAN (2002), $M_o^{\min} = 4.7 \times 10^9$ Nm, are somewhat higher than the laboratory-estimated minimum seismic moment, $M_o^{\min} = 8.5 \times 10^7$ Nm, but within the range of the prediction.

6. Conclusions

If crack growth is involved in earthquake nucleation at some scale, then constitutive equations that describe nucleation should have two components resulting in stable deformation at small inelastic strains (subcritical crack growth) and unstable slip- weakening behavior at large strains (critical crack growth). Laboratory observations from rock fracture and rock friction relevant to earthquake occurrence and earthquake nucleation are consistent with such constitutive equations, as are the predictions of the rate- and state- dependent constitutive formulation specific to rock friction. Considering the detailed rheology of friction and rock fracture as both resulting from crack growth is reasonable and generally expected because fractured rock and highly comminuted wear product are the byproducts of brittle rock deformation. A crack growth-based constitutive equation for earthquake nucleation used with lab-derived constants predicts a minimum earthquake nucleation time on the San Andreas fault of ~ 1 yr. The predicted minimum nucleation patch radius for an earthquake is on the order of 0.2 to 0.06 m and strains associated with nucleation are much too small to be detected by surface or space-borne instruments. The minimum earthquake moment implied by lab observations is $\sim 8.5 \times 10^7$ Nm.

Acknowledgements

Discussions and correspondence with T. Tullis, J. Weeks, J. Dieterich, M. Nakatani, and particularly D. Lockner are gratefully acknowledged. This paper was significantly improved owing to the comments of two anonymous reviewers; many thanks to them and to Peter Mora.

REFERENCES

- ANDREWS, D. J. (1976), *Rupture Propagation with Finite Stress in Antiplane Strain*, J. Geophys. Res. 81, 3575–3582.
- ATKINSON, B. K. and MEREDITH, P. G. (1987), Experimental fracture mechanics data for rocks and minerals. In *Fracture Mechanics of Rock* (B. K. Atkinson ed.), (Academic Press Geology Series, Academic Press, New York, New York), pp. 477–525.

- BEELER, N. M. and LOCKNER, D. L. (2003), *Why Earthquakes Correlate Weakly with the Solid Earth Tides*, J. Geophys. Res., 108, 2391.
- BLANPIED, M. L., MARONE, C. J., LOCKNER, D. A., BYERLEE, J. D., and KING, D. P. (1998). *Quantitative Measure of the Variation in Fault Rheology due to Fluid-rock Interactions*, J. Geophys. Res. 103, 9691–9712.
- BRACE, W. F. and BYERLEE, J. D. (1966), *Stick-slip as a Mechanism for Earthquakes*, Science 153, 990–992.
- CHARLES, R. J. and HILLIG, W. B. (1962), *The kinetics of glass failure by stress corrosion*. In Symposium sur la resistance due verre et les moyens de l'ameliorer, Union Scientifique Continentale du Verr, Charleroi, Belgium, pp. 511–527.
- DAS, S. and SCHOLZ, C. H. (1981), *Theory of Time-dependent Rupture in the Earth*, J. Geophys. Res. 86, 6039–6051.
- DIETERICH, J. H. (1978), *Time-dependent Friction and the Mechanics of Stick Slip*, Pure Appl. Geophys. 116, 790–806.
- DIETERICH, J. H. (1979), *Modeling of Rock Friction. 1, Experimental Results and Constitutive Equations*, J. Geophys. Res. 84, 2161–2168.
- DIETERICH, J. H., *Constitutive properties of faults with simulated gouge*. In *Mechanical Behavior of Crustal Rocks: The Handin Volume*, Geophys. Monogr. Ser., vol. 24 (eds N. L. Carter et al.) AGU, Washington 1981, pp. 103–120.
- DIETERICH, J. H. *A model for the nucleation of earthquake slip*. In *Earthquake Source Mechanics*, Geophys. Monogr. Ser., vol. 37 (eds S. Das et al., (AGU, Washington, D.C. 1986), pp. 37–49.
- DIETERICH, J. H. *Earthquake nucleation on faults with rate- and state-dependent strength*. In *Earthquake Source Physics and Earthquake Precursors* (eds. T. Mikumo et al., Elsevier, New York 1992), pp. 115–134.
- DIETERICH, J. (1994), *A Constitutive Law for Rate of Earthquake Production and its Application to Earthquake Clustering*, J. Geophys. Res. 99, 2601–2618.
- DIETERICH, J. H., and KILGORE, B. D. (1994), *Direct Observation of Frictional Contacts: New Insights for State-dependent Properties*, Pure Appl. Geophys. 143, 283–302.
- DIETERICH, J. H. and KILGORE, B. D. (1996), *Implications of Fault Constitutive Properties for Earthquake Prediction*, Proc. Natl. Acad. Sci., 93, 3787–3794.
- DIETERICH, J., CAYOL, V., and OKUBO, P. (2000), *The Use of Earthquake Rate Changes as a Stress Meter at Kilauea Volcano*, Nature, 408, 457–460.
- GOMBERG, J., BEELER, N. M., BLANPIED, M. L., and BODIN, P. (1998), *Earthquake Triggering by Transient and Static Deformations*, J. Geophys. Res. 103, 24411–24426.
- GRIGGS, D. (1936), *Deformation of Rocks under High Confining Pressure*, J. Geol. 44, 541.
- GU, J., RICE, J. R., RUINA, A. L., and TSE, S. (1984), *Stability of Frictional Slip for a Single Degree of Freedom Elastic System with Nonlinear Rate and State-dependent Friction*, J. Mech. Phys. Solids, 32, 167–196.
- HIRATA, T. (1987), *Omori's Power Law Aftershock Sequences of Microfracturing in Rock Fracture Experiment*, J. Geophys. Res. 92, 6215–6221.
- IDA, Y. (1972), *Cohesive Force Across the Tip of a Longitudinal Shear Crack and Griffith's Specific Surface Energy*, J. Geophys. Res. 77, 3796–3805.
- JOHNSTON, M. J. S. and LINDE, A. T. (2002), *Applications of Crustal Strain during Conventional, Slow, and Silent Earthquakes*, International Handbook of Earthquake seismology, Part A, Elsevier W. Lee editor.
- KNOPOFF, L. (1964), *Earth Tides as a Triggering Mechanism for Earthquakes*, Bull. Seismol. Soc. Am. 54, 1865–1870.
- KNOPOFF, L. (1972), *Model of aftershock occurrence*. In *Flow and Fracture of Rocks*, Geophys. Monograph 16, 259–263.
- KRANZ, R. L. (1980), *The Effects of Confining Pressure and Stress Difference on Static Fatigue of Granite*, J. Geophys. Res. 85, 1854–1866.
- LAWN, B., *Fracture of Brittle Solids* (Cambridge University Press, New York 1993, 378 pp.
- LAPUSTA, N., RICE, J. R., BEN-ZION, Y., and ZHENG, G. (2000), *Elastodynamic Analysis for Slow Tectonic Loading with Spontaneous Rupture Episodes on Faults with Rate- and State-dependent Friction*, J. Geophys. Res. 105, 23765–23789.

- LINKER, M. F. and DIETERICH, J. H. (1992), *Effects of variable normal stress on rock friction: observations and constitutive equations*, J. Geophys. Res. 97, 4923–4940.
- LOCKNER, D. A. (1993), *Room Temperature Creep in Saturated Granite*, J. Geophys. Res. 98, 475–487.
- LOCKNER, D. A. (1998), *A Generalized Law for Brittle Deformation of Westerly Granite*, J. Geophys. Res. 103, 5107–5123.
- LOCKNER, D. A., and OKUBO, P. G. (1983), *Measurements of Frictional Heating in Granite*, J. Geophys. Res. 88, 4313–4320.
- LOCKNER, D. A., BYERLEE, J. D., KUKSENKO, V., PONOMAREV, A., and SIDORIN, A. (1991), *Quasi-static Fault Growth and Shear Fracture*, Nature 350, 39–42.
- LORENZETTI, E. and TULLIS, T. E. (1989), *Geodetic Predictions of a Strike-slip Fault Model: Implications for Intermediate- and Short-term Earthquake Prediction*, J. Geophys. Res. 94, 12,343–12,361.
- MARCELLINI, A. (1995), *Arrhenius Behavior of Aftershock Sequences*, J. Geophys. Res. 100, 6463–6468.
- MARCELLINI, A. (1997), *Physical Model of Aftershock Temporal Behavior*, Tectonophysics, 277, 137–146.
- MCGARR, A. (1994), *Some Comparisons between Mining-induced and Laboratory Earthquakes*, Pure Appl. Geophys. 142, 467–489.
- MCGARR, A. (1999), *On Relating Apparent Stress to the Stress-causing Earthquake Fault Slip*, J. Geophys. Res. 104, 3003–3011.
- MOGI, K. (1962), *Study of Elastic Shocks Caused by the Fracture of Heterogeneous Materials and their Relation to Earthquake Phenomenon*, Bull. Earthquake Res. Inst. Univ. Tokyo 40, 1438.
- MOGI, K. (1974), *On the Pressure Dependence of Strength of Rocks and the Coulomb Fracture Criterion*, Tectonophysics 21, 273–285.
- NAKATANI, M. (2001), *Conceptual and Physical Clarification of Rate and State Friction: Frictional Sliding as a Thermally Activated Rheology*, J. Geophys. Res. 106, 13,347–13,380.
- OKUBO, P. G. and DIETERICH, J. H. (1981), *Fracture Energy of Stick-slip Events in a Large Scale Biaxial Experiment*, Geophys. Res. Lett. 8, 887–890.
- OKUBO, P. G. and DIETERICH, J. H. (1984), *Effects of Physical Fault Properties on Frictional Instabilities Produced on Simulated Faults*, J. Geophys. Res. 89, 5817–5827.
- PALMER, A. C. and RICE, J. R. (1972), *The Growth of Slip Surfaces in the Progressive Failure of Over-consolidated Clay*, Proc. Roy. Soc. Lond. A332, 527–548.
- POWER, W. L., TULLIS, T. E., BROWN, S. R., BOITNOTT, G. N., and SCHOLZ, C. H. (1987), *Roughness of Natural Fault Surfaces*, Geophys. Res. Lett. 14, 29–32.
- REUSCHLE, T. (1990), *Slow Crack Growth and Aftershock Sequences*, Geophys. Res. Lett. 17, 1525–1528.
- RICE, J. R. and RUINA, A. L. (1983), *Stability of Steady Frictional Slipping*, J. Appl. Mech. 50, 343–349.
- RICE, J. R., LAPUSTA, N., and RANJITH, K. (2001), *Rate-and State-dependent Friction on the Stability of Sliding between Elastically Deformable Solids*, J. Mech. Phys. Sol 49, 1865–1898.
- RICHARDSON, E. and JORDAN, T. H. (2002), *Seismicity in Deep Gold Mines of S. Africa: Implications for tectonic Earthquakes*, Bull. Seismol. Soc. Am. 92, 1766.
- RUINA, A. L. (1983), *Slip Instability and State Variable Friction Laws*, J. Geophys. Res. 88, 10,359–10,370.
- SAMMIS, C. G. and STEACY, S. J. (1994), *The Micromechanics of Friction in a Granular Layer*, Pure Appl. Geophys. 142, 777–794.
- SAVAGE, J. C., BYERLEE, J. D., and LOCKNER, D. A. (1996), *Is Internal Friction, Friction?* Geophys. Res. Lett. 23, 487–490.
- Scholz, C., (1968a). The frequency magnitude relation of microfracturing in rock and its relation to earthquakes, Bull. Seismol. Soc. Am. 58, 399.
- SCHOLZ, C. (1968b), *Microfractures, Aftershocks and Seismicity*, Bull. Seismol. Soc. Am. 58, 117–130.
- SCHOLZ, C. H. (1968c), *Mechanism of Creep in Brittle Rock*, J. Geophys. Res. 73, 3295–3302.
- SCHOLZ, C. H. (1972), *Static Fatigue in Quartz*, J. Geophys. Res. 77, 2104–2114.
- TULLIS, T. E. and Weeks, J. D. (1987), *Micromechanics of Frictional Resistance of Calcite*, EOS Trans. Am. Geophys. Un. 68, 405.
- TULLIS, T. E. and WEEKS, J. D. (1986), *Constitutive Behavior and Stability of Frictional Sliding of Granite*, Pure Appl. Geophys. 124, 384–414.
- WEERTMAN, J. (1979), *Inherent Instability of Quasi-static Creep Slippage on a Fault*, J. Geophys. Res. 84, 2146–2152.

- WILCOCK, W. S. D. (2001), *Tidal Triggering of Microearthquakes on the Juan de Fuca Ridge*, Geophys. Res. Lett. 28, 3999–4002.
- WONG, T.-f. *On the normal stress dependence of the shear fracture energy*. In *Earthquake Source Mechanics*, Geophys. Monogr. Ser., vol. 37 (eds. S. Das *et al.*, AGU, Washington, D.C.1986) pp. 1–11.
- YAMASHITA, Y. and KNOPOFF, L. (1987), *Models of Aftershock Occurrence*, Geophys. J. R. astr. Soc. 91, 13–26.
- ZHURKOV, S. N. (1965), *Kinetic Concept of the Strength of Solids*, Int. J. Fracture Mech. 1, 311–323.
- ZHRUKOV, S. N., KUKSENKO, V. S., PETROV, V. A., SAVLYEV, V. N., and SULTANOV, U. (1977), *On the Problem of Prediction of Rock Fracture*, Izv. Acad.Sci. USSR, Phs Solid Earth (in English) 13, 374–379.

(Received September 27, 2002, revised February 28, 2003, accepted March 7, 2003)

To access this journal online:
<http://www.birkhauser.ch>
